Adsorption of cesium from aqueous solution using agricultural residue - walnut shell: Equilibrium, kinetic and thermodynamic modeling studies

Dahu Ding, Yingxin Zhao, Shengjiong Yang, Wansheng Shi, Zhenya Zhang, Zhongfang Lei, Yingnan Yang*

Graduate School of Life and Environmental Sciences, University of Tsukuba, Tsukuba, Ibaraki 305-8572, Japan

* Corresponding author. Graduate School of Life and Environmental Sciences, University of Tsukuba, 1-1-1 Tennodai, Tsukuba, Ibaraki 305-8572, Japan.

Tel.: +81 29-853-4650; Fax: +81 29-853-4650

E-mail address: yo.innan.fu@u.tsukuba.ac.jp (Y. Yang)

Abstract

A novel biosorbent derived from agricultural residue - walnut shell (WS) is reported to remove cesium from aqueous solution. Nickel hexacyanoferrate (NiHCF) was incorporated into this biosorbent, serving as a high selectivity trap agent for cesium. Field emission scanning electron microscope (FE-SEM) and thermogravimetric and differential thermal analysis (TG-DTA) were utilized for the evaluation of the developed biosorbent. Determination of kinetic parameters for adsorption was carried out using pseudo first-order, pseudo second-order kinetic models and intra-particle diffusion models. Adsorption equilibrium was examined using Langmuir, Freundlich and Dubinin-Radushkevich adsorption isotherms. A satisfactory correlation coefficient and relatively low chi-square analysis parameter χ^2 between the experimental and predicted values of the Freundlich isotherm demonstrate that cesium adsorption by NiHCF-WS is a multilayer chemical adsorption. Thermodynamic studies were conducted under

different reaction temperatures and results indicate that cesium adsorption by NiHCF-WS is an endothermic ($\Delta H°>0$) and spontaneous ($\Delta G°<0$) process.

Keywords: Walnut shell; Nickel hexacyanoferrate (NiHCF); Cesium adsorption; Integrated analysis.

1. Introduction

Removal of pollutants from industrial wastewater has become one of the most important issues recently for the increase in industrial activities, especially for heavy metals and radionuclides. Since the big nuclear accident at Fukushima, Japan in 2011, a large amount of radionuclides were released into water, soil and air, and the hazardous influence of radioactive wastewater has drawn much attention all over the world. Among radionuclides, ^{137}Cs is considered the most abundant and hazardous due to diverse sources and relatively long half-life. Furthermore, it can be easily incorporated into terrestrial and aquatic organisms because of its similar chemical characteristics with potassium (Nilchi et al. 2011, Plazinski and Rudzinski 2009). As a result, numerous efforts have been undertaken to find effective and low cost methods to separate and remove cesium (Cs) from waste solutions (Karamanis and Assimakopoulos 2007, Lin et al. 2001, Nilchi et al. 2011, Parab and Sudersanan 2010, Volchek et al. 2011). Generally speaking, the investigated physical-chemical methods for separation and removal of Cs are precipitation, solvent extraction, adsorption, ion exchange, electrochemical and membrane processes (Avramenko et al. 2011, Chen et al. , 2013, Delchet et al. 2012, Duhart et al. 2001, Karamanis and Assimakopoulos 2007, Lin et al. 2001). Among them, solvent extraction, ion exchange and adsorption methods are most widely used. However, due to the high cost of materials, large-scale application of solvent extraction is limited. In the case of ion exchange process, inorganic ion exchangers are found to be superior over organic ion exchangers due to their thermal stability, resistance to ionizing radiation and good compatibility with final waste forms (Nilchi et al. 2002, Plazinski and Rudzinski 2009). Natural occurring clay minerals such as zeolite, bentonite and montmorillonite are usually used as low cost adsorption materials for Cs^+ removal from aqueous solution, however the main disadvantage is the competitive interactions of other monovalent cations, in particular Na^+ and K^+ that can considerably block Cs^+ adsorption (Borai et al. 2009, El-Naggar et al. 2008, Goñi et al. 2006, Lehto 1987, Plazinski and Rudzinski 2009).

Transition metal hexacyanoferrates, especially nickel hexacyanoferrate (NiHCF) is known as a highly selective agent for Cs^+ adsorption (Chen et al. , 2013, Plazinski and Rudzinski 2009). It possesses a special cubic structure with a channel diameter of about 3.2Å, through which only small hydrated ions like Cs^+ can permeate. Larger hydrated

ions like Na^+ get blocked (Plazinski and Rudzinski 2009, Pyrasch et al. 2003). However, the very fine particle size of NiHCF restricts its direct use in practice, thus proper support materials are necessary.

Recently, several kinds of low cost biosorbents have been investigated for the removal of heavy metals (Figueira et al. 2000, Plazinski and Rudzinski 2009, Reddad et al. 2002). Walnut shell, an abundant agricultural residue with good stability has been successfully used in removing heavy metals by adsorption (Altun and Pehlivan 2012, Saadat and Karimi-Jashni 2011, Zabihi et al. 2010). To the best of our knowledge, however, few studies have focused on equilibrium, kinetic and thermodynamic modeling of Cs^+ adsorption using walnut shell. This study presents the first low cost biosorbent derived from walnut shell (WS) as support material incorporated into NiHCF (NiHCF-WS), fabricated for Cs^+ adsorption.

2. Materials and methods

2.1 Materials

Walnut shell used in this study was obtained from Shandong province, China and was immersed and washed with pure water to remove soluble impurities until the water turned clear. The clean WS was completely dried in an oven (EYELA WFO-700, Japan) at 105℃ for more than 24 hours, ground and sieved through No. 8 and 16 size meshes. The granules with diameter between 1~2.36 mm were selected and stored in a desiccator for further use or modification.

2.2 Reagents

The chemicals nickel chloride ($NiCl_2$•$6H_2O$) and potassium hexacyanoferrate ($K_3[Fe(CN)_6]$•$3H_2O$) of A.R. grade were purchased from Wako Pure Chemical Industries Ltd., Japan. Non-radioactive cesium chloride (CsCl) purchased from Tokyo Chemical Industry Co. Ltd., Japan was used as a surrogate for ^{137}Cs because of its same chemical characteristics. All the other reagents used in this study were purchased from Wako Pure Chemical Industries Ltd., Japan with no purification before use. Pure water generated from a Millipore Elix 3 water purification system (Millipore, USA) equipped with a Progard 2 pre-treatment pack was used throughout the experiments except for ICP-MS analysis.

1.26g CsCl was weighed exactly and dissolved into 1L pure water as standard stock Cs^+ solution (1000mg L^{-1}), which could be diluted to desired concentrations of Cs^+ solution for further experiments.

2.3 Modification of walnut shell

The modification of walnut shell contains the following steps. 10 g of clean WS granules were immersed in 100 mL of 50% (v/v%) hydrochloric acid (HCl) for 10 hours at a temperature of 50℃. Then, the WS was dried in an oven at 105℃ overnight after being washed until the eluent pH was almost neutral. The loading of $NiCl_2$ onto WS and the treatment of $K_3[Fe(CN)_6]•3H_2O$ with $NiCl_2$ loaded WS was carried out according to the method reported by Parab and Sudersanan (Parab and Sudersanan 2010). In brief, 5g of WS was immersed in 20mLof 0.5M $NiCl_2•6H_2O$ solution and placed in a double shaker (Taitec NR-30, Japan) at 200 rpm and room temperature (25±1℃) for 24 hours followed by filtration and washing with pure water to remove excess $NiCl_2•6H_2O$. Next, the $NiCl_2$ loaded WS was added to 10mL of 5% (wt%) $K_3[Fe(CN)_6]•3H_2O$ solution and placed into a water bath (SANSYO SWR-281D, Japan) at 30℃ for 24 hours. The resultant NiHCF loaded WS was separated by filtration, washed with pure water and dried at 60℃. The entire procedure was repeated three times to ensure the incorporation of NiHCF onto the WS. This NiHCF-WS material was used for further characterization as well as Cs^+ adsorption studies.

2.4 Kinetic studies

4g of NiHCF-WS was mixed with 200mL Cs^+ solution (adsorbent dosage of 20g L^{-1}) in a 200mL-glass flask (AS ONE, Japan) under initial Cs^+ concentration of 10mg L^{-1}, and the flask was shaken by a double shaker (TAITEC NR-30, Japan) at 200 rpm for 48 hours. Supernatants (about 1mL for each) including the initial solution (as the zero min point) were withdrawn at predetermined time intervals prior to the Cs^+ concentration determination.

In order to investigate the mechanism of adsorption, non-linearized Lagergren pseudo first-order kinetic model (Karamanis and Assimakopoulos 2007) and pseudo second-order kinetic model (Parab and Sudersanan 2010) were applied to analyze the adsorption process, which were expressed as follows:

Lagergren pseudo first-order kinetic model:

$$q_t = q_e(1-e^{-k_1 t}) \qquad (1)$$

pseudo second-order kinetic model:

$$q_t = \frac{k_2 {q_e}^2 t}{1+k_2 q_e t} \qquad (2)$$

where t (min) is the contact time, k_1 (min^{-1}) and k_2 (g mg^{-1} min^{-1}) are the adsorption rate constants; q_e and q_t (mg g^{-1}) represent the uptake amount of ion by the adsorbent at equilibrium and time t, respectively.

In addition, the determination of the limiting step of the adsorption process is necessary by predicting the diffusion coefficient using a diffusion based model. The possibility of intra-particle diffusion resistance affecting the adsorption was explored in this study by using the intra-particle diffusion equation (Delchet et al. 2012) as follows:

$$q_t = k_p t^{1/2} + C \qquad (3)$$

where t (min) is the contact time, q_t (mg g^{-1}) is the Cs^+ uptake amount at time t, k_p (mg g^{-1} $min^{-1/2}$) is the intra-particle diffusion rate constant determined from the slopes of the linear plots. C is the constant, which indicates the thickness of the boundary layer, i.e., the larger the value of C the greater is the boundary layer effect.

2.5 Equilibrium studies

A fixed amount of NiHCF-WS was mixed with 20mL Cs^+ solution in a 50mL-polypropylene tube (VIOLAMO, Japan) at a shaking speed of 200rpm. Resultant supernatants were withdrawn after 24 hours prior to the Cs^+ concentration determination.

2.5.1 Adsorption isotherms

To optimize the design of a adsorption system, it is important to establish the most appropriate correlation for equilibrium conditions (Parab and Sudersanan 2010). According to different adsorption mechanisms, there are currently several different adsorption isotherms used for fitting experimental adsorption results. Among these, Langmuir (Langmuir 1918), Freundlich (Freundlich 1907) and Dubinin-Radushkevich (D-R) (Dubinin et al. 1947) isotherms are widely used and therefore are applied in this study. The nonlinear forms of these isotherms are given as follows:

Langmuir isotherm: $$q_e = \frac{q_m b C_e}{1 + b C_e} \qquad (4)$$

Freundlich isotherm: $$q_e = k_f C_e^{\,n} \qquad (5)$$

D-R isotherm: $$q_e = q_m \exp(-\beta \varepsilon^2) \qquad (6)$$

$$\varepsilon = RT\ln(1+\frac{1}{C_e}) \quad (7)$$

where, q_e (mg g^{-1}) is the amount of Cs^+ adsorbed at equilibrium, C_e (mg L^{-1}) is the equilibrium concentration of Cs^+. b (L mg^{-1}) is a constant related to the free energy or net enthalpy of adsorption ($b \propto e^{-\Delta G/RT}$) (Mohan and Singh 2002), and q_m (mg g^{-1}) is the adsorption capacity at the isotherm temperature. k_f and n are equilibrium constants indicative of adsorption capacity and adsorption intensity respectively. β (mol^2/kJ^2) is the constant related to the adsorption energy, R (8.314J mol^{-1} K^{-1}) is the gas constant and T (K) is the absolute temperature of the aqueous solution.

2.5.2 Role of ion exchange

In the case of anionic metal hexacyanoferrate complexes, it is assumed that there is a true exchange between K^+ and Cs^+ (Haas 1993, Lehto 1987). Therefore, an attempt was made to link the Cs^+ adsorption to its likely ion exchange reaction with K^+ through equilibrium studies. In addition to the batch experiments, a blank experiment was carried out by adding a corresponding amount of adsorbent into the same volume of pure water instead of Cs^+ solutions. The Cs^+ adsorbed and K^+ released was calculated according to mass balance using the equations below:

$$A_{Cs^+} = \frac{(C_0 - C_e)V}{133} \times 1000 \quad (8)$$

where A_{Cs+} (μmol) is the amount of Cs^+ adsorbed by NiHCF-WS, C_0 (mg L^{-1}) is the initial concentration of Cs^+, C_e (mg L^{-1}) is the equilibrium concentration of Cs^+, V (L) is the volume of solution and 133 is the molar mass of Cs.

$$R_{K^+} = \frac{(C_e - C_b)V}{39} \times 1000 \quad (9)$$

where R_{K+} (μmol) is the amount of K^+ released into solution, C_e (mg L^{-1}) is the equilibrium concentration of K^+, C_b (mg L^{-1}) is the concentration of K^+ in the blank solution, V (L) is the volume of solution and 39 is the molar mass of K.

2.6 Thermodynamic studies

In order to obtain the thermodynamic nature of the adsorption process, 0.2g NiHCF-WS was added into 20mL Cs^+ solutions with an initial concentration of 10mg L^{-1} (adsorbent dosage of 10g L^{-1}) at different temperatures (298, 308 and 318K) for 24h. Thermodynamic parameters, namely, standard Gibbs free energy (ΔG°), standard enthalpy (ΔH°) and standard entropy (ΔS°) changes were also determined in order to obtain the thermodynamic nature of the

adsorption process. The amounts of ΔH° and ΔS° could be calculated from the slope and intercept of the straight line obtained from plotting lnKd versus 1/T, respectively using the following equation (Nilchi et al. 2011, Tsai et al. 2009):

$$\ln Kd = \frac{\Delta S^\circ}{R} - \frac{\Delta H^\circ}{RT} \quad (10)$$

where *Kd* (mL g^{-1}) is the distribution coefficient, *R* (8.314J mol^{-1} K^{-1}) is the gas constant and *T* (K) is the absolute temperature of the aqueous solution.

After obtaining ΔH° and ΔS° values of the adsorption, ΔG° of each temperature was calculated by the well-known equation as follows:

$$\Delta G^\circ = \Delta H^\circ - T\Delta S^\circ \quad (11)$$

2.7 Analysis

All of the samples were collected by filtering supernatants through 0.22μm mixed cellulose ester membrane (Millipore, Ireland) and diluted with pure water to a proper extent (below 1mg L^{-1}) into 15mL-polypropylene tubes (VIOLAMO, Japan) prior to inductively coupled plasma-mass spectrometry (ICP-MS) (Perkin Elmer ELAN DRC-e, USA) analysis.

In order to evaluate the probable differences in structure between raw and modified walnut shell, field emission scanning electron microscope (FE-SEM) analysis was performed using a JEOL JSM-6330F type microscope. A thermogravimetric and differential thermal analysis (TG-DTA) of WS and NiHCF-WS was carried out using a thermal analyzer (EXSTAR TG/DTA 7300, Japan) equipped with an AS-3 auto sampler. About 7.5mg of each sample was prepared into an aluminum-PAN, heated up to 500℃ at a constant rate of 10℃ min^{-1} in normal atmosphere for thermal analysis using an open-Al-pan as reference. The whole procedure is shown in Fig.S1 (see Electronic Supplementary Material) during which the air flow rate was kept at 200mL min^{-1}.

The concentrations of Cs^+ and K^+ in aqueous samples were analyzed by a fully quantitative analytical method on a Perkin Elmer ELAN DRC-e ICP-MS in standard mode. Each sample was analyzed 5 times and the average was taken. The relative standard deviation (RSD) of multiple measurements was less than 2% and in most cases, less than 1.5%.

2.8 Calculation

The Cs^+ adsorption results are given as uptake amount (q) and distribution coefficient (Kd). The Cs^+ uptake amount q (mg g^{-1}) was calculated from the mass balance as follows:

$$q = \frac{(C_0 - C_t)V}{1000M} \quad (12)$$

Distribution coefficient Kd (mL g^{-1}), which is mass-weighted partition coefficient between solid phase and liquid supernatant phase reflecting the selectivity for objective metal ions, was calculated according to the formula:

$$Kd = \frac{C_0 - C_t}{C_t} \times \frac{V}{M} \quad (13)$$

where, C_0 and C_t (mg L^{-1}) are the concentrations of Cs^+ at contact time of 0 (initial concentration) and t determined by ICP-MS, V (mL) is the volume of Cs^+ solution and M (g) is the mass of adsorbent used.

2.9 Quality assurance and quality control

In order to ensure reliability and improve accuracy of the experimental data in this study, kinetic and equilibrium studies on Cs^+ adsorption were conducted in duplicate with a mean ±SD being reported. All of the figures and the kinetic fitting displayed in this paper were accomplished using the Origin 7.5 program (OriginLab, USA).

3. Results and discussion

3.1 Characterization of biosorbent

3.1.1 Field emission scanning electron microscope (FE-SEM)

The FE-SEM images of walnut shell before and after modification are shown in Fig.1. It can be seen that the raw walnut shell has a complex and multilayer structure including the obvious fibrous lignocellulosic (Fig.1a). After modification, there is a remarkable difference in the surface structure of walnut shell with NiHCF particles attached on the surface of walnut shell, as depicted by the arrows in Fig.1b.

3.1.2 Thermogravimetric and differential thermal analysis (TG-DTA)

A large number of reactions occur during the thermal degradation of lignocellulosic materials. Therefore, a thermal degradation pre-study conducted on the biomass material, is very important in terms of the efficient design of

thermochemical processes for the conversion of biomass into energy and products (Damartzis et al. 2011). The TG-DTA curves, which display the thermal degradation characteristics for the WS and NiHCF-WS, were recorded as a function of time (Fig.2). Based on the TG curves, it can be said that the major mass loss occurred in the thermal degradation of WS (98.2%) and NiHCF-WS (96.4%), respectively. Their TG curves can be divided into three parts; representing loss of water, volatilation of hemicellulose like contents, and decomposition of celloluse and lignin components (Kar 2011). Compared with WS, the second and last parts of the TG curves obtained from the NiHCF-WS were obviously different with shorter time needed. It can be seen that approximately 37.4% of TG loss occurred during the second part and finished at a time of about 28 minute for the NiHCF-WS. However, the positive peak of the DTA curve was more obvious than that of WS, which might be due to the loss of impurities with lower calorific value than hemicellulose during the modification. Another great difference, the third part began at time of 30 minutes and temperature of about 350℃, much lower than WS, indicating the decomposition temperature greatly decreased after modification. During this step, approximately 52.3% of TG was lost, higher than that of WS.

Through comparing the TG-DTA results of WS and NiHCF-WS, it can be concluded that the modification process didn't alter the thermal stability of WS and therefore NiHCF-WS can be used as a thermally stable adsorbent.

3.2 Effect of contact time and kinetic study

Fig.3 shows the effect of contact time on the Cs^+ adsorption and application of kinetic models to Cs^+ adsorption by WS and NiHCF-WS. Table 1 lists the sorption rate constants associated with pseudo first and second order kinetic models. It can be seen from Fig.3 that Cs^+ adsorption is a rapid process, about 2h is needed to reach equilibrium for the NiHCF-WS. The equilibrium uptake amount of Cs^+ was greater than 0.5mg g^{-1}. In addition, the adsorption process on only-WS is complicated and not efficient with an equilibrium uptake amount of approximately 0.1mg g^{-1}. It is clearly indicated that the NiHCF-WS has a much better adsorption performance for Cs^+ than only-WS.

Compared to the first-order model, the pseudo second-order kinetic model had a higher correlation coefficient for NiHCF-WS, suggesting that the Cs^+ adsorption process is a chemisorption rather than physisorption.

Fig.4 shows the amount of adsorbed Cs^+, q_t (mg g^{-1}), versus the square root of time for NiHCF-WS. The presence of three linear regions on the curve is possibly due to the presence of three steps during the adsorption process (Damartzis et al. 2011): an external mass transfer step such as the boundary layer diffusion occurred first, then an intra-particle diffusion step for the second and lastly a saturation step. In this study, the first linear region with

a high slope signaled a rapid external diffusion stage depicting macro-pore or inter-particle diffusion, which is different from the second step, gradual adsorption stage controlled by intra-particle (micro-pore) diffusion, and the last step (saturation stage). This observation can also be linked with adsorption mechanisms mainly involving the surface layers of crystallites (Ramaswamy 1999).

3.3 Equilibrium studies

3.3.1 Cesium adsorption isotherms

In order to obtain the equilibrium isotherm, the initial Cs^+ concentration varied from 5-400 mg L^{-1} (5, 10, 20, 50, 75, 100, 200, 400) while maintaining an adsorbent dosage of 20g L^{-1}, and the amount of adsorbed Cs^+ was investigated.

Fig.5 shows the application of nonlinear Langmuir, Freundlich and D-R isotherms to the Cs^+ adsorption on NiHCF-WS. In this study, chi-square analysis was applied to estimate the degree of difference (χ^2) between the experimental data and the isotherm data, which is calculated by the following equation (Mirmohseni et al. 2012):

$$\chi^2 = \sum \frac{({q_e}^{\exp} - {q_e}^{cal})^2}{{q_e}^{cal}} \qquad (12)$$

where ${q_e}^{cal}$ (mg g^{-1}) is the equilibrium uptake amount calculated from the isotherm and ${q_e}^{exp}$ (mg g^{-1}) is the experimental equilibrium uptake amount. A smaller χ^2 value indicates a better fitting isotherm.

In addition, the values of normalized standard deviation (NSD (%)) were also calculated to validate the fitness of isotherm to experimental data (Karamanis and Assimakopoulos 2007), which is defined as:

$$\mathrm{NSD}(\%) = 100 \times \sqrt{\frac{\sum[({q_e}^{\exp} - {q_e}^{cal})/{q_e}^{\exp}]^2}{N-1}} \qquad (13)$$

where N is the number of measurements. Similarly, a smaller NSD (%) value indicates a better fitting isotherm.

The results of χ^2 and NSD (%) are given in Table 2 and indicate the three adsorption isotherms match the experimental data (R^2>0.9). Although the R^2 value of the Freundlich isotherm is similar with that of the Langmuir or D-R isotherm, the χ^2 and NSD (%) values of the Freundlich isotherm are much smaller, implying that the adsorption of Cs^+ on NiHCF-WS is a multilayer adsorption rather than monolayer adsorption. Furthermore, the value of n is less than 1, suggesting this adsorption process is favorable (Parab and Sudersanan 2010).

As another important function, the Langmuir isotherm could give us the estimated maximum adsorption capacity (q_m) of NiHCF-WS, 4.94±0.5mg g^{-1}, which is similar to that provided by D-R isotherm. In conclusion, the adsorption isotherms demonstrated that the Cs^+ adsorption onto NiHCF-WS is a multilayer chemical ion exchange process.

3.3.2 Role of ion exchange with K^+

It is hypothesized that if adsorption is mainly caused by ion exchange reaction, then the quantity of the released cations (in gram-equivalent) would be close to that of the adsorbed target ions. Table 3 shows the relationship between the Cs^+ adsorbed and K^+ released during the Cs^+ adsorption process and two significant phenomena are observed. With the increase in dosage (No.1-4) and initial Cs^+ concentration (No.4-7), both Cs^+ adsorbed and K^+ released increase, demonstrating affinity between them. On the other hand, the test results reveal that the amount of K^+ released into solutions are greater than that of Cs^+ adsorbed except for the dosage of 5g L^{-1} (probably caused by experimental error). In other words, the released K^+ from the adsorbent is not completely exchanged by Cs^+ (Avramenko et al. 2011, Loos-Neskovic et al. 2004), which is also in agreement with the relationship between Ca^{2+} released and Cs^+ adsorbed reported by Miah (Miah et al. 2010). This indicates that the amount of K^+ released into the solution is partly through dissolution other than ion exchange with Cs^+. However, it is not clearly demonstrated the existence of chemical ion exchange process between Cs^+ and K^+ from the data reported in this table. Basing on the above conclusion that the existence of dissolution of K^+, as a result, the variations between adsorbed Cs^+ and released K^+ at the same dosage (20g L^{-1}) and different initial Cs^+ concentrations are compared in order to determine the possible equal relationship between them. As a comparison between No.4 and 5, the variation of adsorbed Cs^+ is 8.94±0.07μmol, which is similar with the variation of released K^+ (8.72±0.03μmol). In addition, the variation of adsorbed Cs^+ between No.5 and 6 is 2.01±0.08μmol, which is also similar with the variation of released K^+ (3.31±0.17μmol). When the initial Cs^+ concentration is increased from 200 to 400mg L^{-1} (No.6 and 7), the variation of adsorbed Cs^+ (2.21±0.11μmol) is similar with released K^+ (2.91±0.09μmol). Through the above comparisons, it is consequently concluded that there is indeed an exchange process between Cs^+ and K^+. The K^+ in the NiHCF-WS plays an important role in the Cs^+ adsorption process as the ion exchanger.

3.4 Thermodynamic study

The distribution coefficient *Kd* was calculated using Eq. (13). The plotting of ln*Kd* versus 1/*T* gave a straight line with a correlation coefficient (R^2) of 0.99 (see Fig.S2 in Electronic Supplementary Material), from which the ΔH° and ΔS° was determined using Eq. (10). Furthermore, the standard Gibbs free energy at each temperature was

calculated using Eq. (11) and the results are listed in Table 4.

As shown in Table 4, the distribution coefficient of Cs^+ adsorption by NiHCF-WS increased remarkably with the increase in temperature, implying that high temperature was favorable for Cs^+ adsorption. The same phenomenon was observed by Nilchi et al. (Nilchi et al. 2011), who used copper hexacyanoferrate to adsorb Cs^+ from aqueous solution. The negative amounts of $\Delta G°$ at different temperatures and the positive amount of $\Delta H°$ revealed that the chemical ion exchange process was a spontaneous and endothermic adsorption reaction in this study.

4. Conclusion

Walnut shell, an agricultural residue, was reused as a support material for effective cesium adsorption from aqueous solution and the integrated analysis of adsorption of cesium from aqueous solution using NiHCF-WS was carried out. The rapid adsorption process fitted well with the pseudo second-order kinetic model with the equilibrium cesium uptake amount above 0.5mg g^{-1}. The good correlation coefficient (0.93), low χ^2 and NSD values suggest that cesium adsorption on NiHCF-WS could be best described by the Freundlich adsorption isotherm. Results showed that the NiHCF-WS was an effective adsorbent for cesium adsorption and the adsorption process was endothermic and spontaneous. In addition, the incorporation of walnut shell and NiHCF overcame the difficulty of separation of NiHCF nano-particles from solution. Basing on the conclusions in this study, more effective modification will be carried out to improve the performance of this material and thereafter the evaluation will be performed for the application of this material into treating real radioactive wastewater in future studies.

Acknowledgements

This work was supported in part by Scientific Research (A) 22248075 from the Japan Society for the Promotion of Science (JSPS). The authors also want to give thanks to the Environmental Diplomatic Leader (EDL) writing center, University of Tsukuba, for proofreading.

References

Altun, T. and Pehlivan, E. (2012) Removal of Cr(VI) from aqueous solutions by modified walnut shells. Food Chemistry 132(2), 693-700.

300 Avramenko, V., Bratskaya, S., Zheleznov, V., Sheveleva, I., Voitenko, O. and Sergienko, V. (2011) Colloid stable
301 sorbents for cesium removal: Preparation and application of latex particles functionalized with transition
302 metals ferrocyanides. Journal of Hazardous materials 186(2–3), 1343-1350.
303 Borai, E.H., Harjula, R., malinen, L. and Paajanen, A. (2009) Efficient removal of cesium from low-level radioactive
304 liquid waste using natural and impregnated zeolite minerals. Journal of Hazardous materials 172(1), 416-422.
305 Chen, R., Tanaka, H., Kawamoto, T., Asai, M., Fukushima, C., Na, H., Kurihara, M., Watanabe, M., Arisaka, M. and
306 Nankawa, T. (2013) Selective removal of cesium ions from wastewater using copper hexacyanoferrate
307 nanofilms in an electrochemical system. Electrochimica Acta 87(0), 119-125.
308 Damartzis, T., Vamvuka, D., Sfakiotakis, S. and Zabaniotou, A. (2011) Thermal degradation studies and kinetic
309 modeling of cardoon (Cynara cardunculus) pyrolysis using thermogravimetric analysis (TGA). Bioresource
310 Technology 102(10), 6230-6238.
311 Delchet, C., Tokarev, A., Dumail, X., Toquer, G., Barre, Y., Guari, Y., Guerin, C., Larionova, J. and Grandjean, A.
312 (2012) Extraction of radioactive cesium using innovative functionalized porous materials. RSC Advances
313 2(13), 5707-5716.
314 Dubinin, M.M., Zaverina, E.D. and Radushkevich, L.V. (1947) Sorption and structure of active carbons. I.
315 Adsorption of organic vapors. Zh Fiz Khim 21, 1351-1362.
316 Duhart, A., Dozol, J.F., Rouquette, H. and Deratani, A. (2001) Selective removal of cesium from model nuclear
317 waste solutions using a solid membrane composed of an unsymmetrical calix[4]arenebiscrown-6 bonded to
318 an immobilized polysiloxane backbone. Journal of Membrane Science 185(2), 145-155.
319 El-Naggar, M.R., El-Kamash, A.M., El-Dessouky, M.I. and Ghonaim, A.K. (2008) Two-step method for preparation
320 of NaA-X zeolite blend from fly ash for removal of cesium ions. Journal of Hazardous materials 154(1–3),
321 963-972.
322 Figueira, M.M., Volesky, B., Azarian, K. and Ciminelli, V.S.T. (2000) Biosorption Column Performance with a
323 Metal Mixture. Environmental Science & Technology 34(20), 4320-4326.
324 Freundlich, H. (1907) Über die adsorption in lösungen. Journal of Physical Chemistry 57, 385-470.
325 Goñi, S., Guerrero, A. and Lorenzo, M.P. (2006) Efficiency of fly ash belite cement and zeolite matrices for
326 immobilizing cesium. Journal of Hazardous materials 137(3), 1608-1617.

Haas, P.A. (1993) A Review of Information on Ferrocyanide Solids for Removal of Cesium from Solutions. Separation Science and Technology 28(17-18), 2479-2506.

Kar, Y. (2011) Co-pyrolysis of walnut shell and tar sand in a fixed-bed reactor. Bioresource Technology 102(20), 9800-9805.

Karamanis, D. and Assimakopoulos, P.A. (2007) Efficiency of aluminum-pillared montmorillonite on the removal of cesium and copper from aqueous solutions. Water Research 41(9), 1897-1906.

Langmuir, I. (1918) The adsorption of gases on plane surfaces of glass, mica and platinum. Journal of the American Chemists' Society 40, 1361-1403.

Lehto, J., Harjula, R. (1987) Separation of cesium from nuclear waste solutions with hexacyanoferrate (II)s and ammonium phosphomolybdate. Solvent Extraction and Ion Exchange 5, 343-352.

Lin, Y., Fryxell, G.E., Wu, H. and Engelhard, M. (2001) Selective Sorption of Cesium Using Self-Assembled Monolayers on Mesoporous Supports. Environmental Science & Technology 35(19), 3962-3966.

Loos-Neskovic, C., Ayrault, S., Badillo, V., Jimenez, B., Garnier, E., Fedoroff, M., Jones, D.J. and Merinov, B. (2004) Structure of copper-potassium hexacyanoferrate (II) and sorption mechanisms of cesium. Journal of Solid State Chemistry 177(6), 1817-1828.

Miah, M.Y., Volchek, K., Kuang, W. and Tezel, F.H. (2010) Kinetic and equilibrium studies of cesium adsorption on ceiling tiles from aqueous solutions. Journal of Hazardous materials 183(1–3), 712-717.

Mirmohseni, A., Seyed Dorraji, M.S., Figoli, A. and Tasselli, F. (2012) Chitosan hollow fibers as effective biosorbent toward dye: Preparation and modeling. Bioresource Technology 121(0), 212-220.

Mohan, D. and Singh, K.P. (2002) Single- and multi-component adsorption of cadmium and zinc using activated carbon derived from bagasse—an agricultural waste. Water Research 36(9), 2304-2318.

Nilchi, A., Khanchi, A. and Ghanadi Maragheh, M. (2002) The importance of cerium substituted phosphates as cation exchanger—some unique properties and related application potentials. Talanta 56(3), 383-393.

Nilchi, A., Saberi, R., Moradi, M., Azizpour, H. and Zarghami, R. (2011) Adsorption of cesium on copper hexacyanoferrate–PAN composite ion exchanger from aqueous solution. Chemical Engineering Journal 172(1), 572-580.

Parab, H. and Sudersanan, M. (2010) Engineering a lignocellulosic biosorbent – Coir pith for removal of cesium from aqueous solutions: Equilibrium and kinetic studies. Water Research 44(3), 854-860.

355 Plazinski, W. and Rudzinski, W. (2009) Modeling the Effect of Surface Heterogeneity in Equilibrium of Heavy Metal
356 Ion Biosorption by Using the Ion Exchange Model. Environmental Science & Technology 43(19),
357 7465-7471.
358 Pyrasch, M., Toutianoush, A., Jin, W.Q., Schnepf, J. and Tieke, B. (2003) Self-assembled films of Prussian blue and
359 analogues: Optical and electrochemical properties and application as ion-sieving membranes. Chemistry of
360 Materials 15(1), 245-254.
361 Ramaswamy, M. (1999) Synthesis, Sorption and Kinetic Characteristics of Silica-Hexacyanoferrate Composites.
362 Solvent Extraction and Ion Exchange 17(6), 1603-1618.
363 Reddad, Z., Gerente, C., Andres, Y. and Le Cloirec, P. (2002) Adsorption of Several Metal Ions onto a Low-Cost
364 Biosorbent: Kinetic and Equilibrium Studies. Environmental Science & Technology 36(9), 2067 -2073.
365 Saadat, S. and Karimi-Jashni, A. (2011) Optimization of Pb(II) adsorption onto modified walnut shells using factorial
366 design and simplex methodologies. Chemical Engineering Journal 173(3), 743-749.
367 Tsai, S.-C., Wang, T.-H., Li, M.-H., Wei, Y.-Y. and Teng, S.-P. (2009) Cesium adsorption and distribution onto
368 crushed granite under different physicochemical conditions. Journal of Hazardous materials 161(2–3),
369 854-861.
370 Volchek, K., Miah, M.Y., Kuang, W., DeMaleki, Z. and Tezel, F.H. (2011) Adsorption of cesium on cement mortar
371 from aqueous solutions. Journal of Hazardous materials 194(0), 331-337.
372 Zabihi, M., Haghighi Asl, A. and Ahmadpour, A. (2010) Studies on adsorption of mercury from aqueous solution on
373 activated carbons prepared from walnut shell. Journal of Hazardous materials 174(1–3), 251-256.

374
375

Graphic abstract:

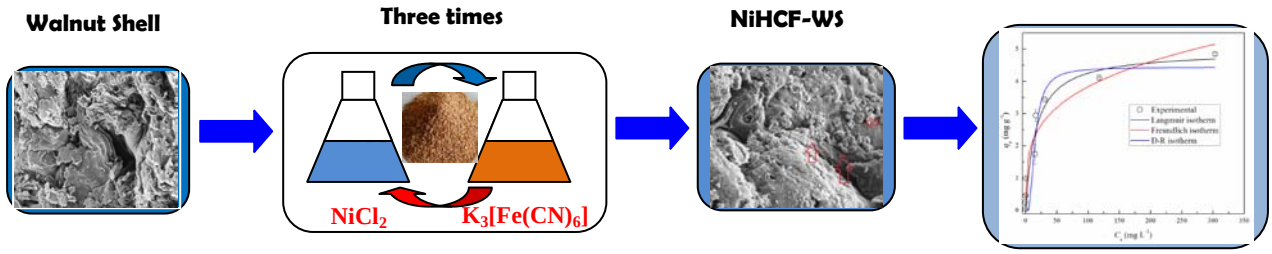

Fig. 1

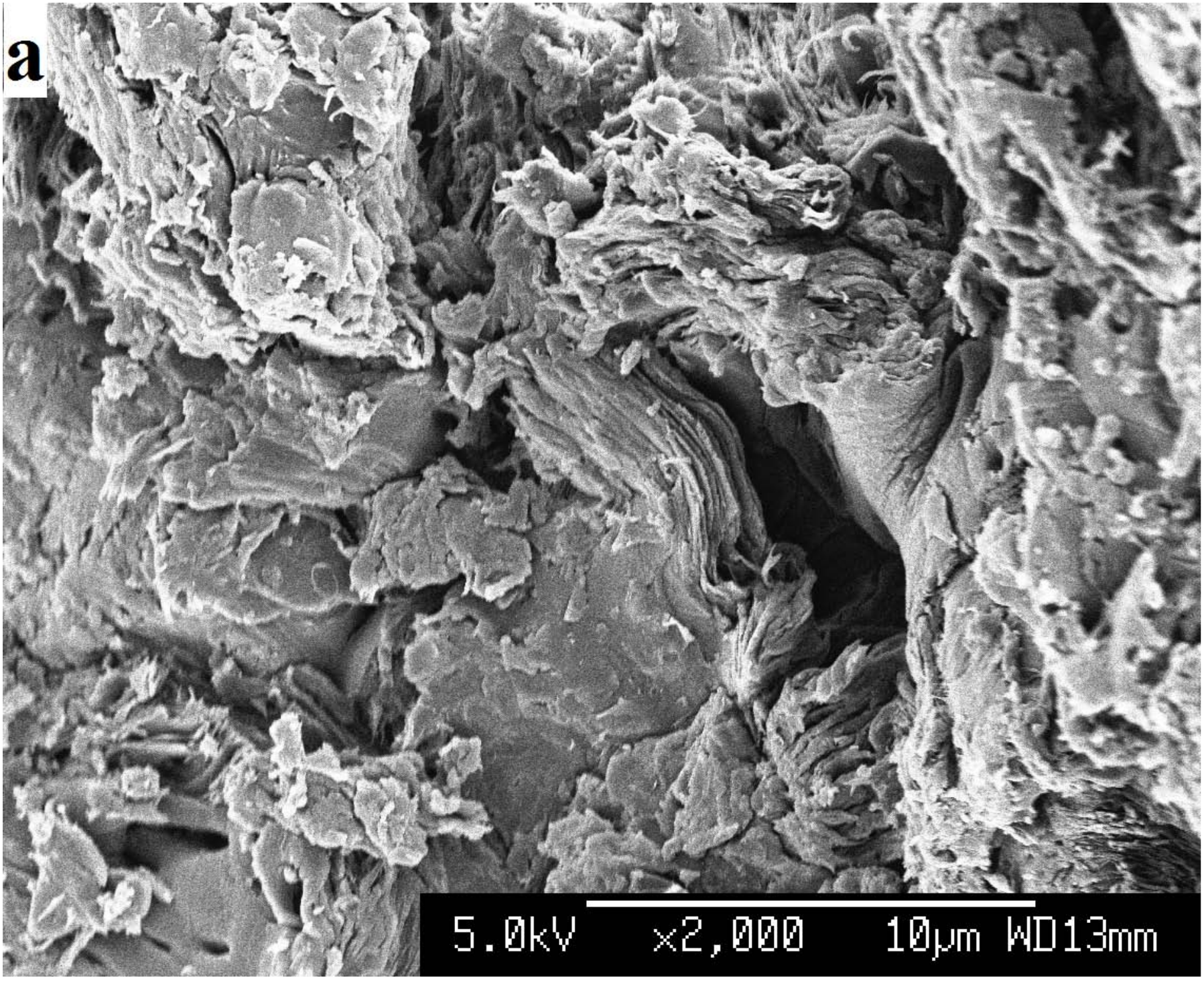

Fig. 1

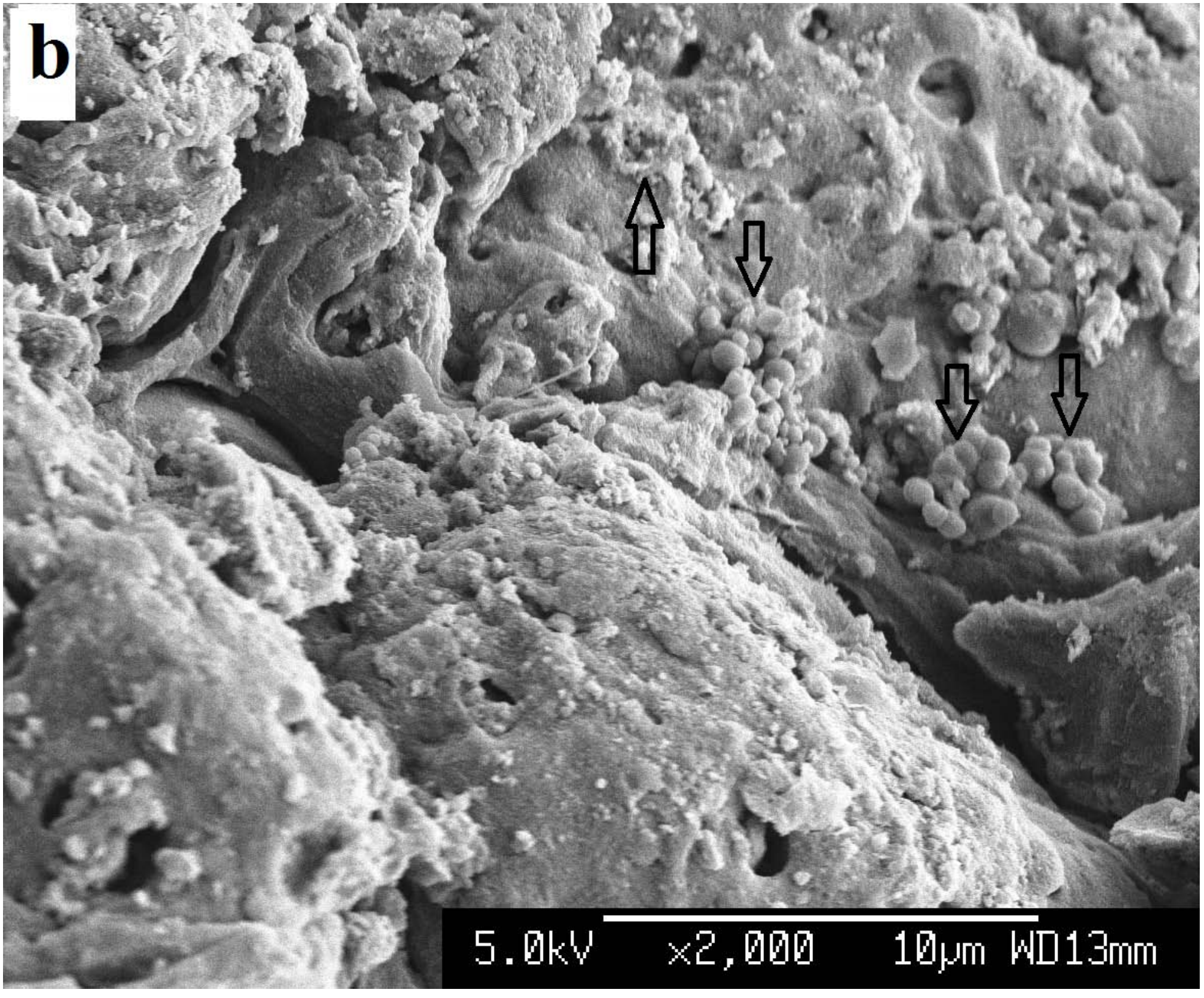

Fig. 2(1)

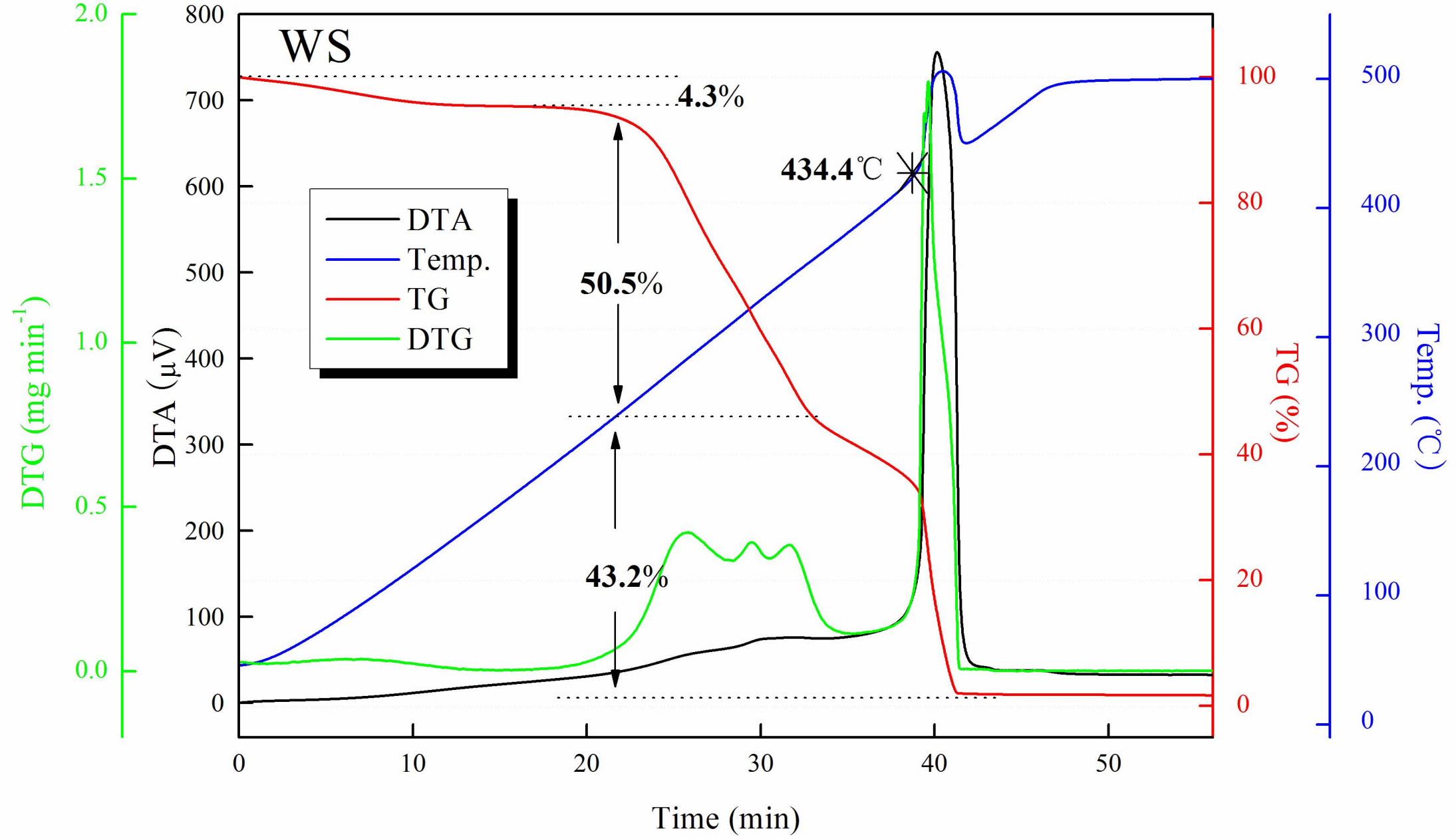
WS
4.3%
434.4℃
50.5%
43.2%
DTA
Temp.
TG
DTG
DTG (mg min-1)
DTA (μV)
TG (%)
Temp. (℃)
Time (min)
0
10
20
30
40
50
0.0
0.5
1.0
1.5
2.0
0
100
200
300
400
500
600
700
800
0
20
40
60
80
100
0
100
200
300
400
500

Fig. 2(2)

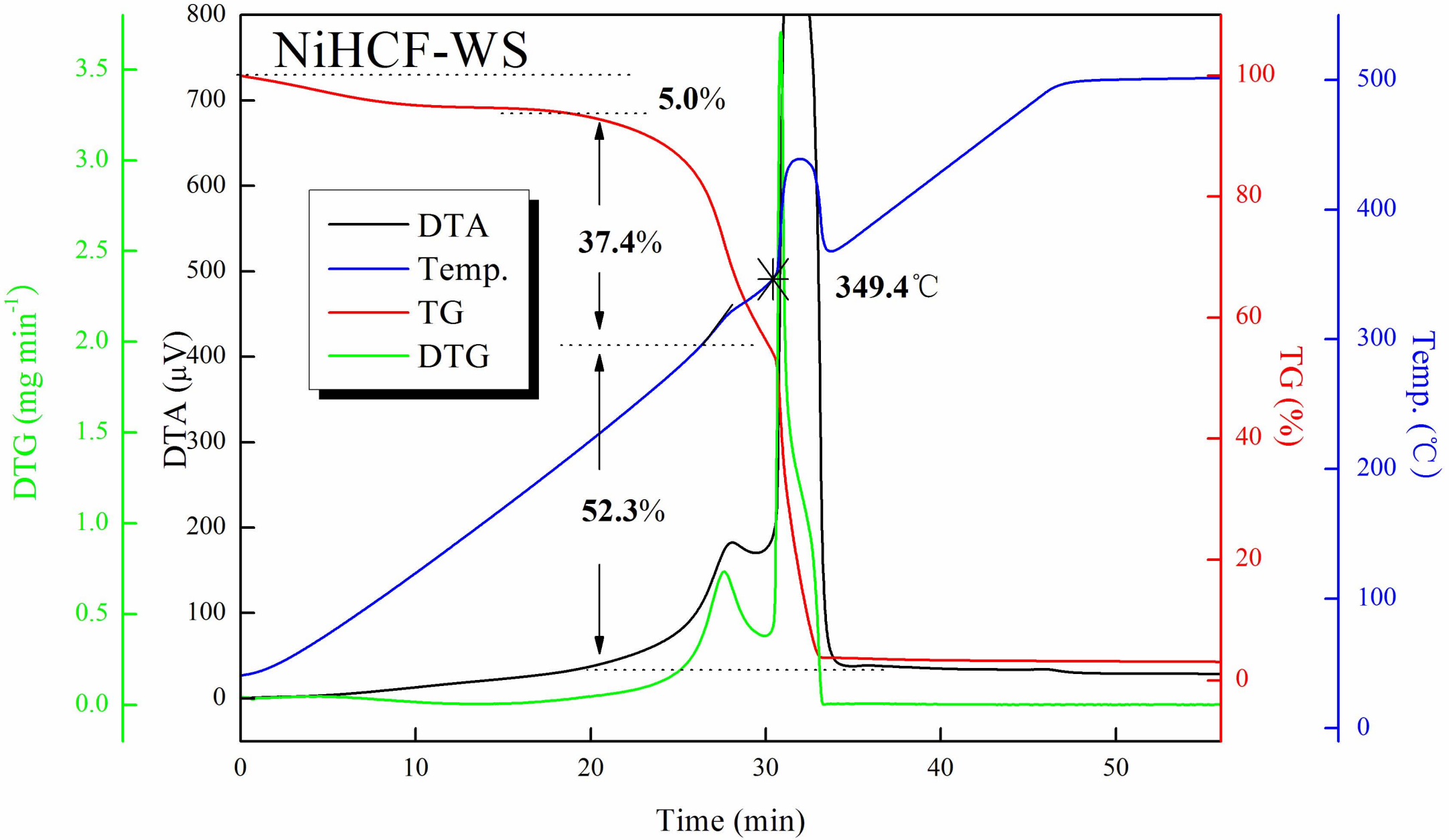
NiHCF-WS
5.0%
37.4%
52.3%
349.4℃
DTA
Temp.
TG
DTG
DTG (mg min-1)
DTA (μV)
TG (%)
Temp. (℃)
Time (min)
0.0
0.5
1.0
1.5
2.0
2.5
3.0
3.5
0
100
200
300
400
500
600
700
800
0
20
40
60
80
100
0
100
200
300
400
500
0
10
20
30
40
50

Fig. 3

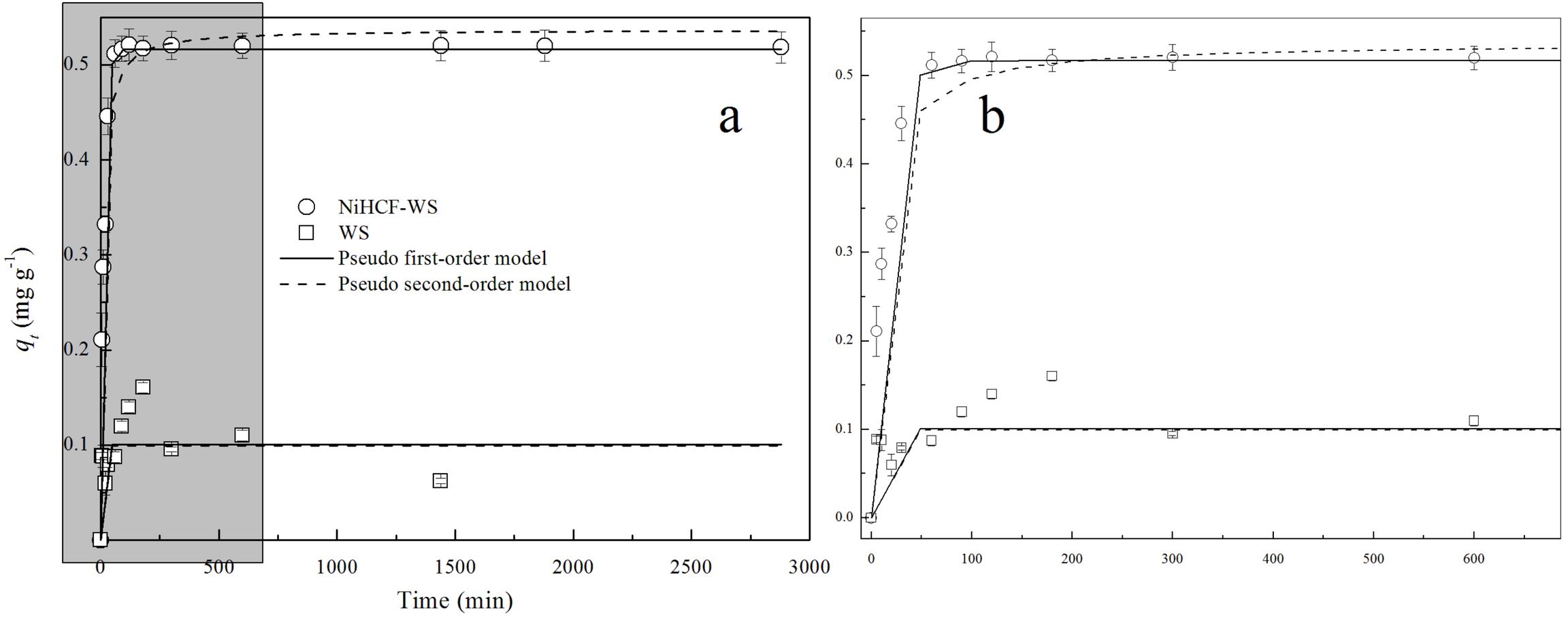
a
b
NiHCF-WS
WS
Pseudo first-order model
Pseudo second-order model
q_t (mg g^{-1})
Time (min)
0
0.1
0.2
0.3
0.4
0.5
0
500
1000
1500
2000
2500
3000
0.0
0.1
0.2
0.3
0.4
0.5
0
100
200
300
400
500
600

Fig. 4

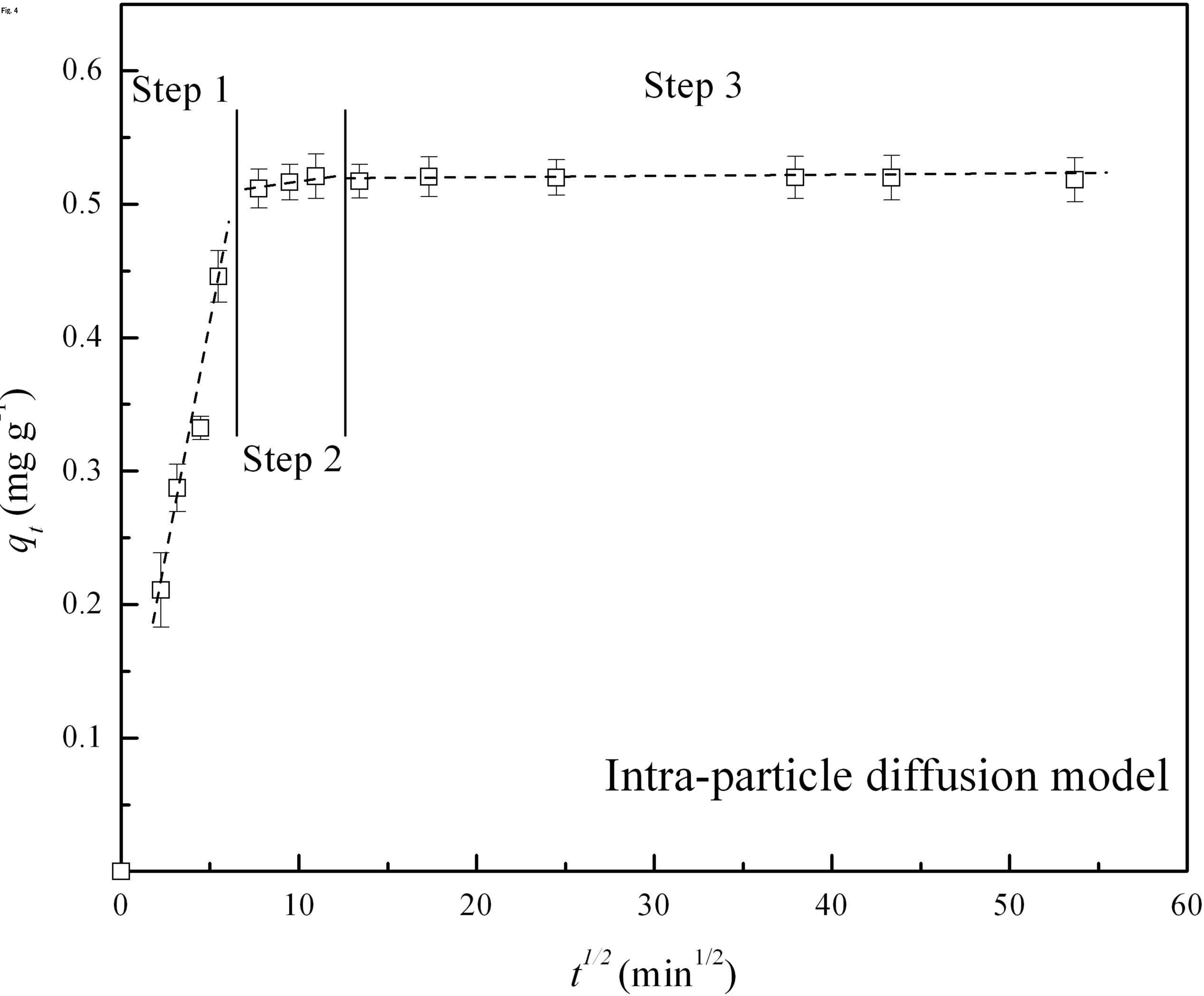
Step 1
Step 2
Step 3
Intra-particle diffusion model
q_t (mg g^{-1})
$t^{1/2}$ (min$^{1/2}$)
0.1
0.2
0.3
0.4
0.5
0.6
0
10
20
30
40
50
60

Fig. 5

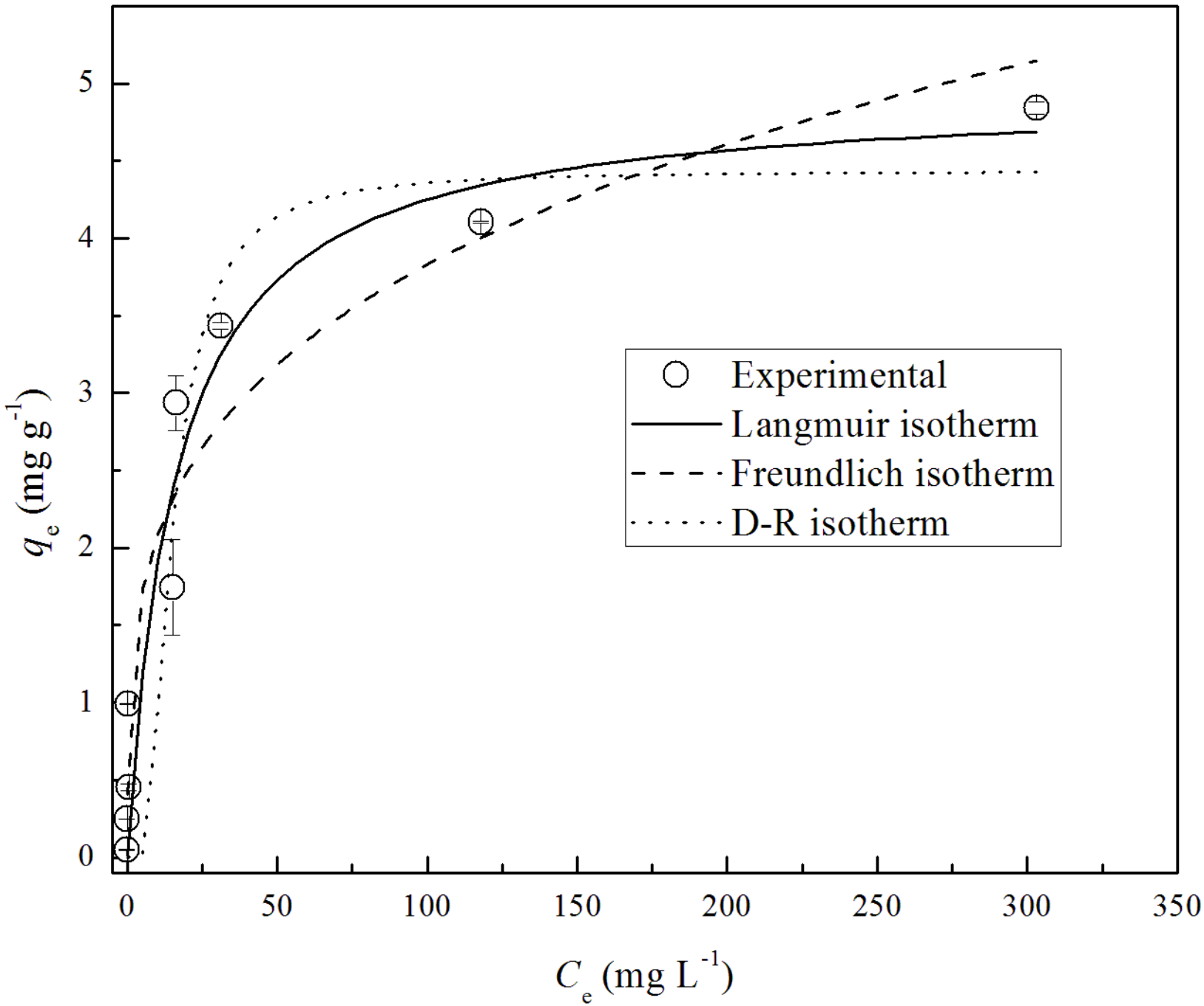
Experimental
Langmuir isotherm
Freundlich isotherm
D-R isotherm
q_e (mg g^{-1})
C_e (mg L^{-1})
0
1
2
3
4
5
0
50
100
150
200
250
300
350

Fig. S1

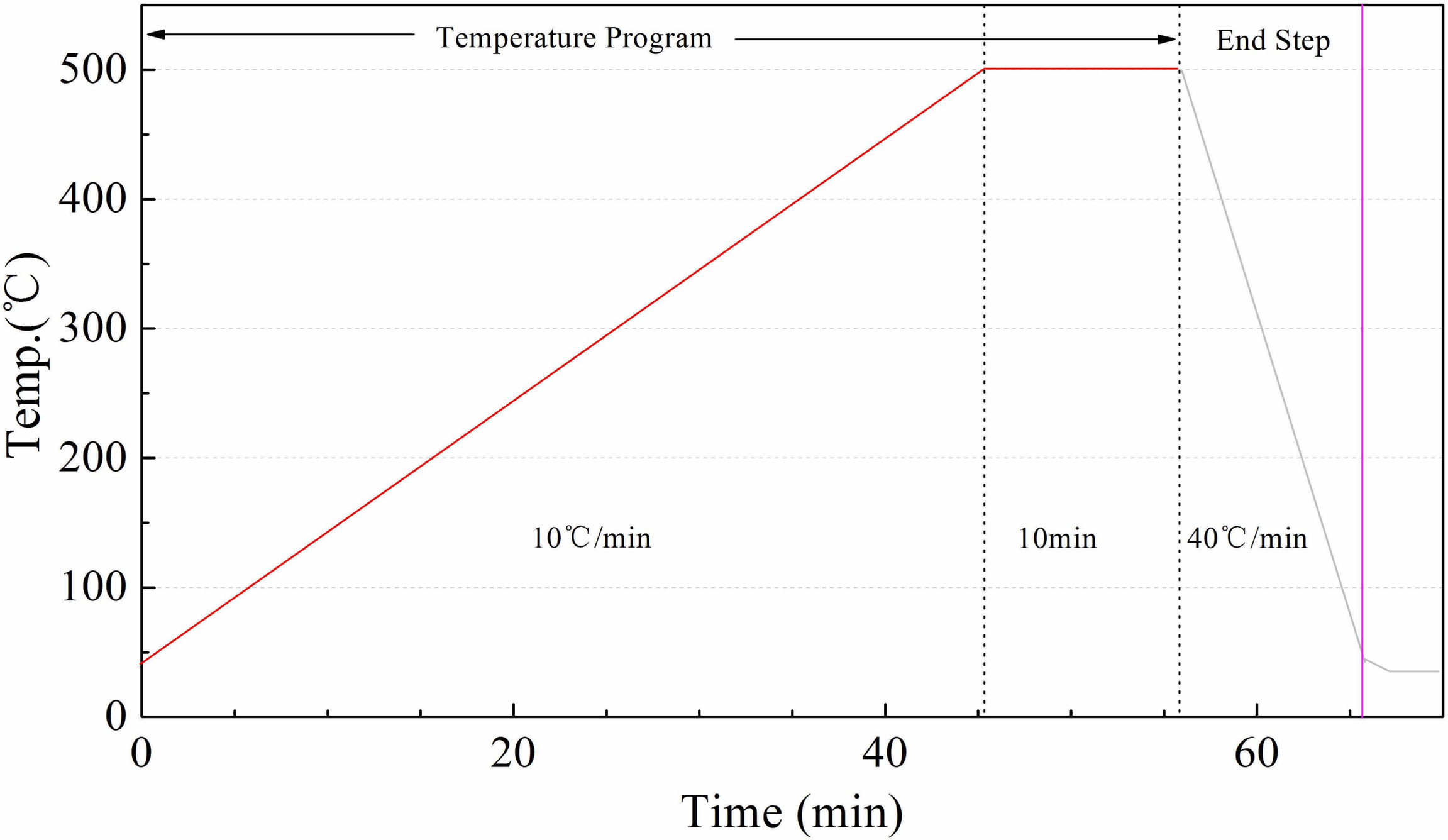
Temperature Program
End Step
500
400
300
200
100
0
Temp.(℃)
0
20
40
60
Time (min)
10℃/min
10min
40℃/min

Fig. S2

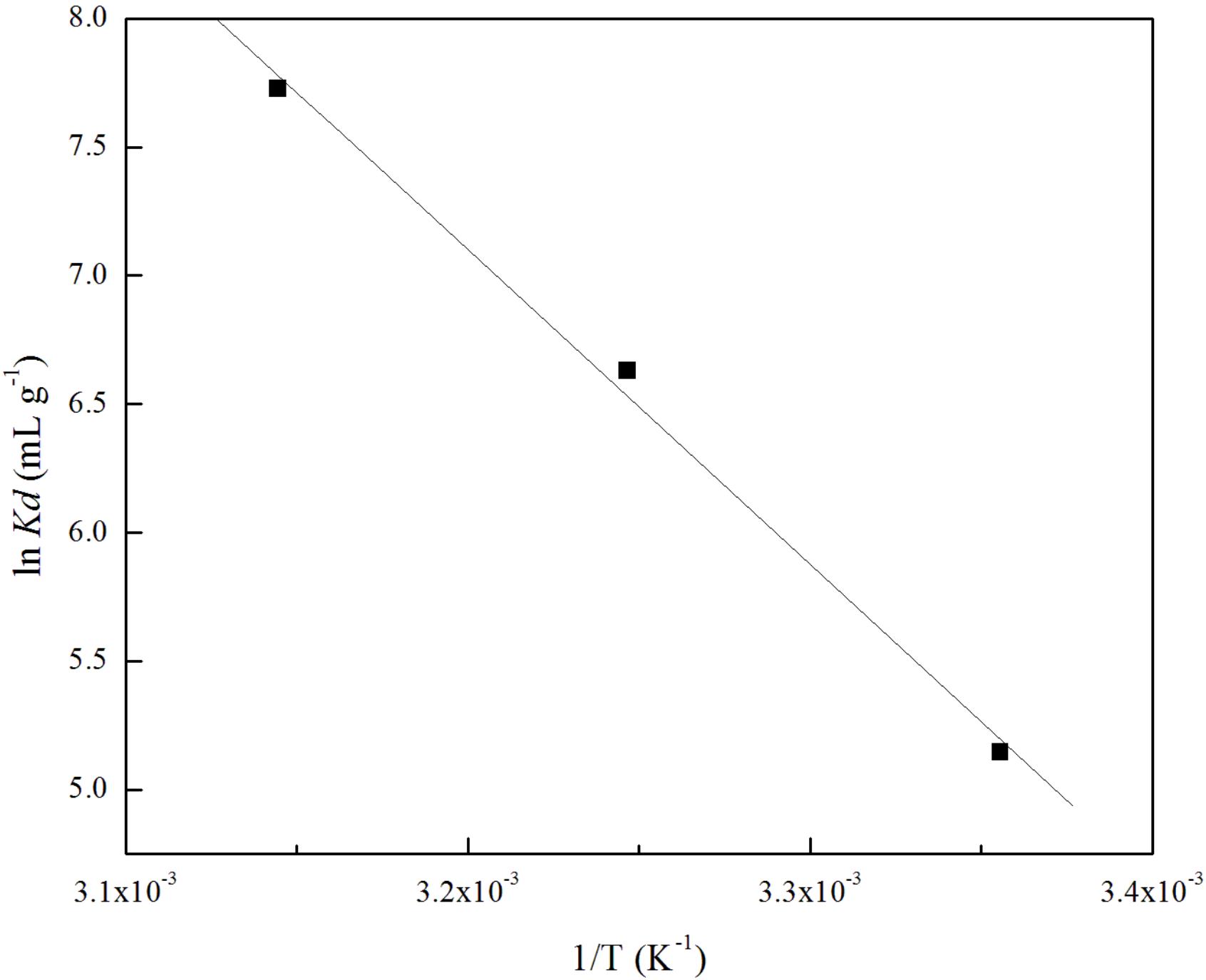
8.0
7.5
7.0
6.5
6.0
5.5
5.0
ln Kd (mL g-1)
3.1x10-3
3.2x10-3
3.3x10-3
3.4x10-3
1/T (K-1)

Figure captions:

Fig.1 – Typical scanning electron microscope images of walnut shell before (a) and after (b) modification. (Acceleration voltage of 5.0kV and 2000× magnification, arrows show the nickel hexacyanoferrate particles)

Fig.2 – TG-DTA results of walnut shell and nickel hexacyanoferrate incorporated walnut shell obtained at the heating rate of 10℃ min^{-1} in air atmosphere. (Pan: Al-Pan; Reference: Open-Al-Pan; Upper limit temperature: 550℃; Gas flow rate: 200mL min^{-1})

Fig.3 – Application of non-linearized pseudo first (solid line) and second (dash line) order kinetic models for cesium (10mg L^{-1}) adsorption by walnut shell (square) and nickel hexacyanoferrate incorporated walnut shell (circle) at 25℃ (20g L^{-1}). (Fig.(b) shows the enlarged dark part in Fig.(a).)

Fig.4 – Intra-particle diffusion model of cesium (10mg L^{-1}) adsorption by nickel hexacyanoferrate incorporated walnut shell (20g L^{-1}) at 25℃. (Symbols represent the experimental data.)

Fig.5 – Nonlinear Langmuir (solid line), Freundlich (dash line) and D-R (dot line) isotherms of cesium adsorption on nickel hexacyanoferrate incorporated walnut shell at 25℃. (Symbols represent the experimental data, whereas the lines represent the simulated data fitted using the adsorption isotherms.)

Fig. S1 – Temperature program of TG-DTA analysis. (Red line represents the temperature program and only during this period the experimental data are recorded. Gray line shows the end step with a speed of 40℃ min^{-1} and as said, the experimental data are not recorded during this step.)

Fig. S2 – Effect of solution temperature on the distribution coefficient of cesium (10mg L^{-1}) adsorption by NiHCF-WS (10g L^{-1}) (R^2=0.99).

Table 1

Pseudo first-order kinetic model			Pseudo second-order kinetic model		
	WS	NiHCF-WS		WS	NiHCF-WS
q_{eexp} [a] (mg g^{-1})	0.11±0.04	0.52±0.004	q_{eexp} (mg g^{-1})	0.11±0.04	0.52±0.004
k_1 (min^{-1})	0.37±0.39	0.071±0.006	k_2 (g mg^{-1} min^{-1})	(-3.8±4.0)×10^{45}	0.23±0.03
q_{ecal} [b] (mg g^{-1})	0.10±0.01	0.52±0.009	q_{ecal} (mg g^{-1})	0.099±0.01	0.54±0.01
R^2	0.492	0.946	R^2	0.483	0.981

[a] means the equilibrium sorption capacity estimated from the experimental data.

[b] means the equilibrium sorption capacity calculated from the kinetic model.

Table 2

Langmuir isotherm		Freundlich isotherm		D-R isotherm	
q_m (mg g^{-1})	4.94±0.5	k_f (mg g^{-1} $L^{1/n}$ $mg^{-1/n}$)	1.12±0.2	q_m (mg g^{-1})	4.43±0.4
b (L mg^{-1})	0.06±0.02	n	0.27±0.04	β (mol^2/kJ^2)	$(3±0.8)\times10^{-5}$
R^2	0.93	R^2	0.93	R^2	0.92
χ^2	21.1	χ^2	0.96	χ^2	1.3×10^{281}
NSD (%)	57.3	NSD (%)	60.7	NSD (%)	310.2

Table 3 [a]

No.	Dosage ($g\ L^{-1}$)	Initial Cs^+ concentration ($mg\ L^{-1}$)	Cs^+ adsorbed (μmol)	K^+ released (μmol)
1	5	10	0.5±0.02	0.1±0.0
2	10	10	0.9±0.002	1.5±0.06
3	15	10	1.4±0.001	4.6±0.3
4	20	10	1.4±0.001	4.7±0.2
5	20	100	10.3±0.07	13.4±0.2
6	20	200	12.3±0.01	16.7±0.02
7	20	400	14.6±0.1	19.6±0.1

[a] Samples were tested in 50mL polypropylene tubes with 20mL Cs^+ solutions at room temperature and 200rpm for 24h.

Table 4

Temp. (K)	*Kd* (mL g^{-1})	ΔG° (kJ mol^{-1})	ΔH° (kJ mol^{-1})	ΔS° (kJ K^{-1} mol^{-1})
298	171.4	−12.9		
308	757.1	−16.8	101.8	0.385
318	2264.3	−20.6		